Rapid *in Vitro* Assembly Dynamics and Subunit Turnover of FtsZ Demonstrated by Fluorescence Resonance Energy Transfer*

Yaodong Chen and **Harold P. Erickson**‡

From the Department of Cell Biology, Duke University Medical Center, Durham, North Carolina 27710

Abstract

We have developed an assay for the assembly of FtsZ based on fluorescence resonance energy transfer (FRET). We mutated an innocuous surface residue to cysteine and labeled separate pools with fluorescein (donor) and tetramethylrhodamine (acceptor). When the pools were mixed and GTP was added, assembly produced a FRET signal that was linearly proportional to FtsZ concentration from 0.7 µM (the critical concentration (C_c)) to 3 µM. At concentrations greater than 3 µM, an enhanced FRET signal was observed with both GTP and GDP, indicating additional assembly above this second C_c. This second C_c varied with Mg^{2+} concentration, whereas the 0.7 µM C_c did not. We used the FRET assay to measure the kinetics of initial assembly by stopped flow. The data were fit by the simple kinetic model used previously: monomer activation, a weak dimer nucleus, and elongation, although with some differences in kinetic parameters from the L68W mutant. We then studied the rate of turnover at steady state by pre-assembling separate pools of donor and acceptor protofilaments. When the pools were mixed, a FRET signal developed with a half-time of 7 s, demonstrating a rapid and continuous disassembly and reassembly of protofilaments at steady state. This is comparable with the 9-s half-time for FtsZ turnover *in vivo* and the 8-s turnover time of GTP hydrolysis *in vitro*. Finally, we found that an excess of GDP caused disassembly of protofilaments with a half-time of 5 s. Our new data suggest that GDP does not exchange into intact protofilaments. Rather, our interpretation is that subunits are released following GTP hydrolysis, and then they exchange GDP for GTP and reassemble into new protofilaments, all on a time scale of 7 s. The mechanism may be related to the dynamic instability of microtubules.

FtsZ, a homolog of tubulin, is the major protein of the bacterial cell division machine. Light microscopy shows that FtsZ assembles into a Z-ring that constricts to divide the cell. The Z-ring is highly dynamic *in vivo*. Subunits in the ring continuously exchange with a half-time of 8–9 s (1,2). *In vitro*, FtsZ assembles into single-stranded protofilaments, which are thought to be the basic assembly unit making up the Z-ring.

We recently developed a tryptophan fluorescence assay for FtsZ assembly using the mutant FtsZ-L68W (3). The tryptophan fluorescence of this mutant increased 2.5-fold upon assembly. A major advantage of this assay is that it accurately reports total polymer, in contrast to centrifugation and light scattering, which underreport small polymers. The tryptophan fluorescence assay was used for a comprehensive study of the kinetics of initial assembly. The

Note Added in Proof—We would like to reference two previous studies showing that excess GDP caused a rapid disassembly of FtsZ (25,26). We suggest that the GDP-induced disassembly reflects the steady-state turnover rate in both of these cases.

data were fit to a model involving a step of monomer activation and formation of a weak dimer nucleus followed by elongation steps that were thermodynamically more favorable.

The critical concentration (C_c) of the mutant FtsZ-L68W was 5–10-fold lower than that of wild-type FtsZ, meaning that it assembled with higher affinity. The mutant protein does, however, function normally for cell division, so we believe the basic assembly mechanism is the same as for wild-type FtsZ. Nevertheless, we felt it was important to study nucleation and elongation of a protein closer to wild type. We therefore designed a new fluorescence assay based on fluorescence resonance energy transfer (FRET). [1] The FRET assay requires two pools of subunits, one labeled with a donor fluorophore (fluorescein) and the other with an acceptor (tetramethylrhodamine (TMR)). When the subunits assemble into a protofilament, they will assort randomly, and a significant fraction of donors will be adjacent to an acceptor. The 4.3-nm spacing of subunits in the FtsZ protofilament (4) is smaller than the 5.0 –5.5-nm Förster distance of a fluorescein-TMR pair (5,6), so the FRET signal should provide a direct measure of total subunits in polymer.

To label FtsZ for FRET, we constructed the mutant FtsZ-F268C, which introduces a single cysteine on the lower back right surface (7). F268C was originally identified as a mutant that was resistant to the division inhibitor SulA (8). It functions normally for cell division (8), and its rate of GTP hydrolysis is only slightly reduced (7). In the crystal structure of an FtsZ-SulA complex, it is seen that Phe-268 makes contact with SulA, consistent with the mutation blocking the binding of SulA (9). However, Phe-268 is ~2 nm from the protofilament interface (10), so it should have minimal or no effect on protofilament assembly. Leu-68, in contrast, makes partial contact across the interface, and the larger tryptophan probably enhances assembly by contributing additional area to the interface.

In addition to providing a measure of the initial assembly kinetics, the FRET assay provides a novel approach to measure the dynamics of subunit turnover at steady state.

MATERIALS AND METHODS

Protein Purification

The mutant F268C of *Escherichia coli* FtsZ was overexpressed from a pET11b vector (Novagen). The protein was purified using the protocol of Romberg *et al.* (11) with some modifications. Following the 20% ammonium sulfate cut and 30% precipitation, the protein was chromatographed on a Resource Q 10/10 column (Amersham Biosciences) with a linear gradient of 50–500 m$_M$ KCl in 50 m$_M$ Tris, pH 7.9, 1 m$_M$ EDTA, 10% glycerol. Peak fractions were identified by SDS-PAGE and stored frozen at -80 °C.

---

[1]The abbreviations used are:

FRET

fluorescence resonance energy transfer

TMR

tetramethylrhodamine

Mes

4-morpholineethanesulfonic acid

EM

electron microscopy

GMP-CPP

guanosine 5′-(α,β-methylene)triphosphate.

Protein Labeling

Fluorescein-5-maleimide and tetramethylrhodamine-5-maleimide were purchased from Molecular Probes. FtsZ-F268C protein in 50 m$_M$ Tris, pH 7.9, 200 m$_M$ KCl was reacted with a 5-fold excess of probe for 2 h at room temperature. The protein was dialyzed against 50 m$_M$ Mes, pH 6.5, 2.5 m$_M$ MgAc, 1 m$_M$ EGTA to remove free probe, and KCl (KCl prevents the efficient pelleting of calcium polymers). Before each experiment, a cycle of calcium assembly-disassembly (12) was done to remove any inactive protein and remaining free probe. CaCl$_2$ was added to 10 m$_M$ and GTP to 2 m$_M$, and the reaction was incubated 5 min at 37 °C. The FtsZ polymer was collected by centrifugation at 45,000 rpm for 30 min (Beckman TLA100 rotor). The pellet was resuspended in the appropriate buffer at a protein concentration >100 μ$_M$. The sample was centrifuged again to remove any insoluble protein. The protein concentration was determined using a BCA assay (Pierce) and corrected for the 75% color ratio of FtsZ/BSA (13). To measure the TMR-labeled protein, the BCA assay was read at 655 nm instead of the usual 570 nm (where TMR absorbs).

The labeling efficiency was ~60–90% for each fluorophore. Higher labeling should give a stronger FRET signal, but the exact ratio of fluorophore to FtsZ was not important for these measurements. Experimentally, we found that different ratios of the labels and variable amounts of unlabeled subunits gave different FRET levels, but the kinetics were the same. One experiment gave identical kinetics when one-half of the labeled protein was replaced with unlabeled FtsZ. This shows that the labeled FtsZ has similar assembly properties to unlabeled FtsZ.

Electron Microscopy Measurements

Negative stain electron microscopy was used to visualize FtsZ filaments. About 10 μl of FtsZ solution was incubated with GTP for several minutes and applied to a carbon-coated copper grid. Excess solution was blotted with filter paper, and the grid, held at a 50° angle, was rinsed with 3–4 drops of 2% uranyl acetate, blotted, and air-dried. Filaments were visualized and photographed using a Phillips 301 electron microscope at x50,000 magnification.

Fluorescence Measurement

FRET can be measured by the increase in acceptor fluorescence, the decrease in donor fluorescence, or the ratio. For the kinetic measurements, we wanted to measure at a single wavelength, and we chose the decrease in donor fluorescence, which gave a much stronger signal than the acceptor increase.

Steady-state fluorescence spectra were measured using a Shimadzu RF-5301 PC spectrofluorometer. The samples measured included donor only (FtsZ labeled with fluorescein plus unlabeled FtsZ equivalent to that with acceptor), donor plus acceptor FtsZ without GTP, and donor plus acceptor FtsZ with 200 μ$_M$ GTP. The donor-acceptor ratio was ~2:3. All samples were excited at 470 nm, and the fluorescence spectra were recorded from 480 to 650 nm. For kinetic measurements, donor emission was measured at 516 nm.

Stopped-flow measurements were made using an SLM-Aminco 8100 spectrofluorometer equipped with the SLM Milliflow reactor stopped-flow accessory. The temperature was controlled at 25 °C. The donor fluorescence was excited at 470 nm, and the emission intensity was monitored at 516 nm, both with a 4-nm slit. The protein concentration was initially calculated based on the dilution and was adjusted so that the initial fluorescence values fell on a straight line.

For measurements of assembly kinetics, the FtsZ donor and acceptor were mixed at a ratio of 2:3 and then rapidly mixed with an equal volume of 500 μ$_M$ GTP to initiate the reaction. To

measure the rate of subunit exchange at steady state, donor FtsZ and acceptor FtsZ at 3–10 μ_M were first assembled separately by adding 1 m_M GTP, and then these two pools were rapidly mixed and exchanged.

Most assembly experiments were done in MMK buffer (50 m_M Mes, 100 m_M KAc, 5 m_M MgAc, 1 m_M EGTA, pH 6.5). Two other buffers, HMK (50 m_M Hepes, pH 7.7, 100 m_M KAc, 5 m_M MgAc, 1 m_M EGTA) and MEK (50 m_M Mes, 100 m_M KAc, 2.5 m_M EDTA, 1 m_M EGTA, pH 6.5), were used as noted.

Kinetic Modeling

The FtsZ assembly kinetics data were fitted using the minimal kinetic model described previously (3). Three steps followed the addition of GTP to FtsZ: activation of the FtsZ monomer, formation of a dimer nucleus, and elongation (Scheme I). (Note that the kinetic constants for the elongation steps (k_3—k_8) are all identical, except k_{-7}, which is set to zero; see Ref. 3 for the rationale.) The kinetic data were fit using the programs KINSIM40 and FITSIM40 (14-17).

RESULTS

The Critical Concentration of FtsZ-F268C Determined by the FRET Assay

When donor (fluorescein) FtsZ co-assembles with acceptor (TMR) FtsZ, the donor fluorescence should decrease and acceptor fluorescence should increase. We found that the donor fluorescence at 516 nm decreased up to 40% when 6 μ_M FtsZ (mixed donor and acceptor) was induced to assemble by adding GTP (Fig. 1a). Acceptor fluorescence at 575 nm showed a corresponding increase, but this was a smaller signal. Moreover, fluorescence at 575 nm is complicated by a substantial contribution from donor emission, which decreases because of FRET and subtracts from the acceptor increase. We have therefore used the decrease in donor fluorescence as the best FRET signal.

We plotted the donor fluorescence *versus* FtsZ concentration for donor only, donor-acceptor without GTP, and donor-acceptor with GTP. At concentrations <0.7 μ_M, the three curves superimposed, meaning there was no FRET and no assembly. When concentrations were >0.7 μ_M, the GTP curve showed a decrease in donor fluorescence that was linear with FtsZ concentration. This indicates a C_c of 0.7 μ_M for the GTP assembly in the lower concentration range.

There was, however, a surprising observation that at FtsZ concentrations >3 μ_M, a FRET signal developed simply from mixing the donor and acceptor FtsZ without any GTP. We assumed that the FtsZ carries a stoichiometric amount of GDP (following assembly and disassembly in Ca^{2+}), and we found that adding excess GDP did not change the curve, so we refer to this as GDP-mediated assembly. This FRET signal only occurred at concentrations of >3 μ_M total FtsZ (at the 5 m_M Mg^{2+} in our standard MMK buffer) (Fig. 1c). The FRET signal appeared to be linear above 3 μ_M, suggesting that it is reporting a second cooperative assembly with a 3 μ_M C_c. This C_c, dependent on the concentration of Mg^{2+}, was 4, 3, or 2 μ_M in 2.5, 5, and 10 mM Mg^{2+}, respectively (Fig. 1, *b-d*). In the absence of Mg^{2+}, we found no FRET signal up to 10 μ_M FtsZ. We show results for MMK, pH 6.5, but very similar curves were obtained in HMK (pH 7.7), with a C_c of 4.2 μ_M in 5 m_M Mg^{2+} (not shown).

Even more surprising, the curves for GTP assembly showed a second break at the same C_c for each Mg^{2+} concentration, suggesting that GTP assembly is characterized by two C_cs. We used electron microscopy (EM) to look for a structural basis for the enhanced FRET at the higher concentrations. EM showed apparently normal, single protofilaments at 2 μ_M FtsZ (Fig. 2a). Fig. 2c shows the distribution of protofilament lengths, with an average of about 120 nm or 30

subunits. The distribution of filament lengths was virtually identical at 10 μ_M FtsZ, although at the higher concentration, some protofilaments further associated into pairs and small bundles (Fig. 2*b*). This distribution is addressed under "Discussion."

FtsZ Assembly Kinetics Measured by FRET

Fig. 3 shows the kinetics of assembly when the FtsZ donor-acceptor mixture was mixed with 0.5 m$_M$ GTP in MMK buffer using a stopped-flow device. All assembly curves showed a lag of 2–3 s, a decrease over 6–10 s, and finally a plateau. The assembly kinetics curves from 0.8 to 3 μ_M were fit to the kinetic model in Scheme I using the programs KINSIM40 and FITSIM40. Because the FRET signals are complicated by the GDP-mediated oligomerization at a higher concentration, we did not include data over 3 μ_M in the fitting. These kinetics were fit to the same scheme as the kinetics of FtsZ-L68W, namely a weak dimer nucleus followed by elongation. The major difference was a much weaker dimer nucleus, which is discussed below (Table I).

Assembly kinetics in HMK buffer at pH 7.7 were almost identical to the kinetics in MMK at pH 6.5 (Table I). We also measured the kinetics of the GDP assembly by mixing separate pools of donor and acceptor at 10 μ_M. The donor fluorescence decreased rapidly and was at a plateau in 200 ms.

Rapid Steady-state Subunit Turnover

We used the FRET assay to measure the rate of protofilament turnover at steady state. For this step, we first assembled donor FtsZ and acceptor FtsZ separately. These assembled pools were then mixed rapidly in the stopped-flow device, and the FRET signal was measured as the decrease in donor fluorescence. This FRET signal requires that the subunits disassemble from the separately labeled protofilaments and reassemble into mixed donor-acceptor protofilaments. In MMK buffer, the donor fluorescence decreased rapidly to a plateau (Fig. 4*a*). The data were fit well by a single exponential, $F = F_{eq} + \alpha \cdot e^{-t/\tau}$. The reaction time τ was 9.3 s, which corresponds to a half-time of 7 s. At steady state, protofilament disassembly must be balanced by reassembly of new protofilaments, so this number measures the rate of each reaction. Thus this experiment shows that all protofilaments are disassembling and reassembling on the time scale of 9 s. The turnover rate was essentially the same for FtsZ concentrations from 3 to 10 μ_M. The fluorescence decrease was 30%, essentially the same as the 33% decrease for the initial assembly. This means that the turnover involved complete disassembly and reassembly of all protofilaments.

To examine the turnover rate in the absence of GTP hydrolysis, we repeated the experiment in MEK buffer, where the chelation of Mg^{2+} permits protofilament assembly but blocks GTP hydrolysis (3,18). After the mixing, the donor fluorescence decreased, and again the decrease could be fit to a single exponential (Fig. 4*b*). However, there were two differences from the assembly in Mg^{2+}. First, the final decrease in fluorescence was only 12% in EDTA *versus* 30% in Mg^{2+}. This suggests that only about one-third of the subunits participate in exchange in EDTA. Second, the reaction time was 127 s in EDTA *versus* 9.3 s in Mg^{2+}. We believe the exchange in EDTA is consistent with reversible dissociation and re-association of subunits at the protofilament ends, with no turnover in the middle.

Finally, we repeated the mixing experiment with protofilaments assembled in 0.2 m$_M$ GMP-CPP. In this case, the mixing appeared to approach completion, but the reaction time was increased to 350 s. This is consistent with the previous observation that GMP-CPP is hydrolyzed 3–10-fold more slowly than GTP (11).

Rate of FtsZ Depolymerization with Added Excess GDP

Excess GDP can cause FtsZ depolymerization. To observe the kinetics of disassembly, we first assembled 3–10 μM mixed FtsZ (ratio of donor to acceptor was 1:1) in 100 μM GTP. GDP was added to 2 mM, and the sample was rapidly mixed by pipette. Fig. 5, *a* and *b*, shows the time course of donor fluorescence increase as the protofilaments disassembled. The reaction time for the exponential fit was 6 ± 1 s in MMK buffer (Fig. 5*a*) and 25 ± 5 s in MEK buffer (Fig. 5*b*).

We also examined the disassembly of the tryptophan mutant, FtsZ-L68W, monitoring the change in tryptophan fluorescence (Fig. 5*c*). The average lifetime of this decay was about 8 s in MMK buffer and 125 s in MEK buffer. The slower disassembly of L68W in MEK buffer is consistent with the 5–10-fold lower k_{-e} of L68W relative to F268C, but it could also reflect differences in filament length.

We checked the effect of adding smaller amounts of GDP to protofilaments. In MEK buffer with 200 μM GTP, the addition of 100 and 200 μM GDP caused disassembly of 40 and 60% of the polymer. In MMK buffer, 200 μM GDP caused disassembly of 30% of the polymer. If we assume that GTP and GDP compete for binding and that subunits are inactivated when they have bound GDP, these results suggest that the affinity of FtsZ is somewhat higher for GDP in EDTA and somewhat higher for GTP in Mg^{2+} buffer. This is very different from tubulin, where the affinity for GDP is ~3-fold lower than for GTP in Mg^{2+} and GTP binding is hardly measurable in EDTA (19).

DISCUSSION

Kinetics and Steady-state Assembly in GTP

The kinetics of initial assembly measured here by FRET were fit to the same model (Scheme I) used to fit the assembly of the tryptophan mutant, FtsZ-L68W (3). The model involves a step of monomer activation (probably the time needed for release of the initially bound GDP), the formation of a weak dimer nucleus, and a stronger association-giving elongation.

One concern in the previous study was that the C_c of the L68W mutant was about 5–10-fold smaller than that of wild-type FtsZ. The labeled protein used for the present FRET assay showed a C_c of 0.7 μM in steady-state measurements (Fig. 1, *b—d*) and 0.5–0.6 μM from kinetics (k_{-e}/k_e, Table I). This is very close to the C_cs of 0.9–1.25 μM measured by sedimentation for wild-type FtsZ (3) and 0.5 μM from GTPase (20). Furthermore, adding an equal amount of unlabeled FtsZ reduced the magnitude of the FRET signal but did not change the kinetics of assembly (not shown). Thus we believe that the assembly of labeled F268C is essentially identical to that of wild-type FtsZ.

The kinetic constants for F268C and L68W are compared in Table I. The interpretation of the kinetic constants is discussed in detail by Chen *et al.* (3). The major difference is that the dimer nucleus is much weaker for F268C than for L68W assembly. The K_D for the dimer, given by k_{-2}/k_2, is about 500-fold larger than the K_D for elongation, k_{-e}/k_e for F268C, *versus* only a 2.5–10-fold difference for L68W in Mg^{2+} buffers. Thus the kinetic evidence for a cooperative assembly is even stronger than it was for L68W. As discussed in more detail by Chen *et al.* (3), we still have no mechanism to explain how a protofilament that is 1 subunit thick can exhibit the characteristics of cooperative assembly and a dimer nucleus.

The plot of the steady-state FRET signal *versus* FtsZ concentration gave the expected results in MMK for FtsZ concentrations up to 3 μM (in our standard buffer with 5 mM Mg^{2+}). Below the C_c of ~0.7 μM, there was no FRET signal, and above this C_c, the donor fluorescence showed a linear decrease from 0.7 to 3 μM FtsZ. This FRET signal indicates a GTP-mediated assembly,

which we interpret to be the straight, single-stranded protofilaments seen in Fig. 2a and in previous EM studies. It should be noted that this C_c for GTP assembly was about 0.7 μM at all Mg^{2+} concentrations (from 2.5 to 10 mM), implying that this assembly does not involve binding of additional Mg^{2+}.

As we pointed out previously (3), the simple model used to fit the kinetic data ignores the role of GTP hydrolysis. Because hydrolysis occurs only slowly following entry of a subunit into the protofilament (20), the nucleation and initial elongation phases should not be affected. At steady state, however, the apparent k_{-e}, which determines the apparent C_c, will mostly be because of dissociation of subunits following GTP hydrolysis, with a smaller contribution from dissociation of FtsZ-GTP. Unfortunately, at the present time we do not know where to place GTP hydrolysis in a kinetic scheme, so the mechanism must remain incomplete. Our confidence in the overall scheme, and in particular the dimer nucleus, is supported by our previous study of assembly in EDTA, which demonstrated similar cooperative assembly without the complication of GTP hydrolysis (3).

A Second Critical Concentration

An important new discovery of the FRET assay is a Mg^{2+}-sensitive assembly pathway with a second C_c. FtsZ-GDP showed an abrupt and linear FRET signal (decrease in donor fluorescence) above 3 μM FtsZ (in 5 mM Mg^{2+}). Sedimentation studies have already demonstrated an assembly of FtsZ-GDP into dimers and small oligomers (21,22), and this assembly was Mg^{2+}-dependent, similar to our results with the FRET assay. A major difference between our results and the previous sedimentation assays is that we found an abrupt transition to assembly above a C_c, whereas the previous studies were interpreted as a gradual isodesmic assembly. The C_c implies that assembly in GDP is cooperative, not isodesmic. We suggest that the sedimentation results might be reinterpreted as a cooperative assembly, with all subunits above the C_c incorporated into small oligomers of a similar length.

Remarkably, the second C_c was not just a phenomenon of GDP-mediated assembly but was also observed in all curves for GTP assembly. This second decrease in slope always occurred at the same C_c that was observed for GDP assembly. One possibility for this second step of GTP assembly is that it represents bundling of protofilaments. Indeed our EM analysis did show some bundling at higher protein concentrations. However, there are several problems with this interpretation. First, even at 10 μM FtsZ, the large majority of protofilaments are not bundled. Second, it is difficult to understand why bundling would exhibit a C_c, rather than a more gradual concentration dependence. Third, there is no explanation as to why this second C_c was the same in GDP and in GTP assembly. At present, we do not understand the mechanism of this second step of cooperative assembly.

No such additional break was seen in our previous study using the tryptophan fluorescence of L68W. This is understandable because the tryptophan fluorescence change is mediated only by the longitudinal contacts within the protofilament and is not likely to be affected by lateral association. The discovery of this second association was only possible with the FRET assay.

Steady-state Polymer Dynamics

A second important use of the FRET assay was to investigate assembly dynamics at steady state. This was not possible with any previous assay, including tryptophan fluorescence. We mixed preformed protofilaments labeled separately with donor and acceptor and found that they developed a FRET signal with a half-time of 7 s. This means that the pre-assembled protofilaments are completely disassembling and reassembling with this rapid half-time. This is very close to the 8–9 s half-time for FtsZ turnover in the Z-ring *in vivo* (2) and also to the rate of GTP hydrolysis *in vitro* (8/min in MMK (20) and 14/min in HMK (23)). This agreement

of the turnover kinetics suggests that *in vitro* assembly is indeed close to the *in vivo* reaction, and both appear to be regulated by GTP hydrolysis.

This turnover rate implies a balance of protofilament disassembly and reassembly. We decided to test it further by looking at one side of the turnover, disassembly. To rapidly block assembly, we added an excess of GDP, which should replace the GTP on all free monomers and block their assembly into new protofilaments. As monomers disassemble, they presumably already have a bound GDP, and the excess prevents them from getting a GTP. The disassembly was somewhat faster than the steady-state turnover time, with a half-time of 5 s *versus* 7 s for turnover. This would be expected if the concurrent reassembly sometimes rescued protofilaments that would otherwise disassemble completely. This disassembly rate is also consistent with the $k_{-e} = 3.5$ s^{-1} that we obtained from kinetics data (Table I). At this rate, a protofilament of the average length of 30 subunits would disassemble completely in 8.5 s.

The GDP-induced disassembly also addresses the issue of whether nucleotide can exchange within a protofilament. It was suggested previously that this might be possible and necessary to explain the high turnover rate of GTP hydrolysis (24). Recently a crystal structure of an FtsZ dimer showed a gap in the interface that might permit nucleotide exchange (10). We now believe that this is unlikely for three reasons. 1) Our new data show that the turnover rate of subunits at steady state (half-time, 7 s) is fully fast enough to accommodate GTP hydrolysis (8/min = 7.5 s/GTP hydrolyzed). 2) When we suddenly added excess GDP to assembled protofilaments, it caused disassembly with a half-time of 5 s, fully consistent with the normal disassembly rate during turnover. 3) When we added GDP to protofilaments assembled in EDTA, they disassembled at a much slower rate, consistent with their slower turnover. If GDP could displace GTP in assembled protofilaments, this should happen on a faster time scale, probably equivalent to the 1–3-s lag seen in the initial assembly kinetics. Overall, our data suggest a model wherein subunits need to disassemble to exchange the GDP for GTP and initiate a new round of assembly. This is similar to the mechanism of tubulin turnover.

This turnover rate also correlates nicely with the measured lengths of protofilaments. EM showed protofilaments averaging about 30 subunits (Fig. 2*c*). The initial assembly kinetics for elongation are diffusion-limited, with $k_e = 6.6$ μM^{-1}s^{-1} (Table I). At steady state, the free monomer concentration should be 0.7 μM, so monomers can add to the protofilament at a rate of $6.6 \times 0.7 = 4.6$ s^{-1}. A protofilament that is 30 subunits long could therefore be assembled in 6.5 s. Longer protofilaments would not be possible with the observed turnover rate. The Z-ring *in vivo*, which has a circumference of ~3,000 nm, shows the same turnover rate. We conclude that the Z-ring is built from overlapping segments of short protofilaments ~120 nm in length.

We found that the distribution of protofilament lengths was the same at 2 and 10 μM total FtsZ. This independence of protofilament length on FtsZ concentration is expected from the rapid turnover. After 1–2 min of assembly, every protofilament will have turned over several times. Importantly, every reassembly will occur from the pool of free subunits at a concentration of 0.7 μM. Thus, higher concentrations of total FtsZ will produce more protofilaments of the same length.
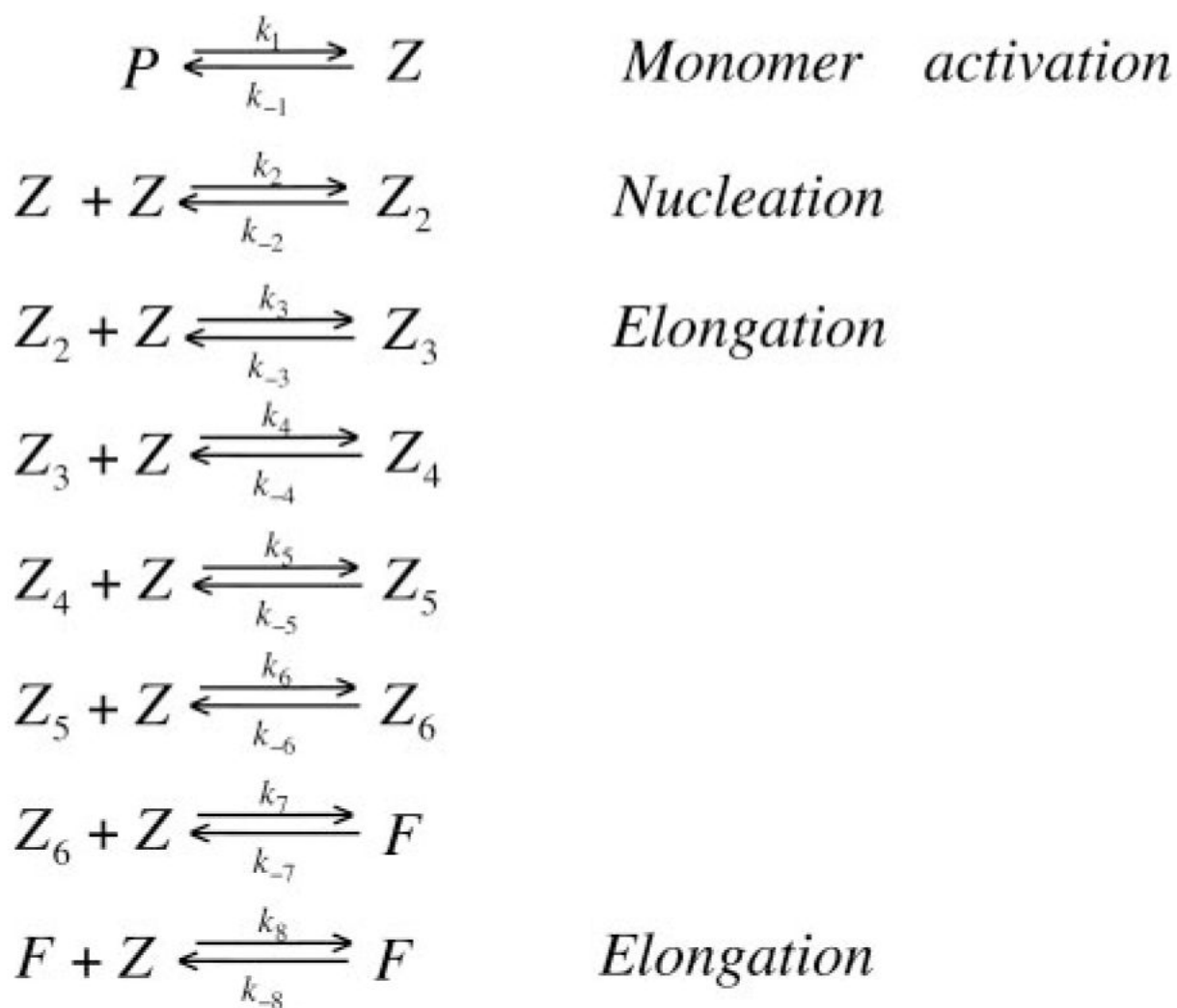
Finally, the *in vitro* experiment provides new insight on the *in vivo* exchange into the Z-ring. The exchange *in vivo* could have been because of exchange of individual subunits or of whole protofilaments. The *in vitro* FRET experiment can only be explained by exchange of subunits, probably by dissociation and reassociation at protofilament ends. This suggests that the *in vivo* exchange, which has the same half-time, also occurs by exchange of individual subunits.

In conclusion, we suggest speculatively that the rapid assembly dynamics may operate by a mechanism related to dynamic instability of microtubules. Novel experimental approaches may

be needed to explore the mechanism. The FRET assay described here provides one new tool for these future experiments.

REFERENCES

1. Stricker J, Maddox P, Salmon ED, Erickson HP. Proc. Natl. Acad. Sci. U. S. A 2002;99:3171–3175. [PubMed: 11854462]

2. Anderson DE, Gueiros-Filho FJ, Erickson HP. J. Bacteriol 2004;186:5775–5781. [PubMed: 15317782]

3. Chen Y, Bjornson K, Redick SD, Erickson HP. Biophys. J 2005;88:505–514. [PubMed: 15475583]

4. Erickson HP, Stoffler D. J. Cell Biol 1996;135:5–8. [PubMed: 8858158]

5. Corbalan-Garcia S, Teruel JA, Gomez-Fernandez JC. Eur. J. Biochem 1993;217:737–744. [PubMed: 8223616]

6. Glauner KS, Mannuzzu LM, Gandhi CS, Isacoff EY. Nature 1999;402:813–817. [PubMed: 10617202]

7. Lu C, Stricker J, Erickson HP. BMC Microbiol 2001;1:7. [PubMed: 11394965]

8. Bi E, Lutkenhaus J. J. Bacteriol 1990;172:5602–5609. [PubMed: 2145263]

9. Cordell SC, Robinson EJ, Lowe J. Proc. Natl. Acad. Sci. U. S. A 2003;100:7889–7894. [PubMed: 12808143]

10. Oliva MA, Cordell SC, Lowe J. Nat. Struct. Mol. Biol 2004;11:1243–1250. [PubMed: 15558053]

11. Romberg L, Simon M, Erickson HP. J. Biol. Chem 2001;276:11743–11753. [PubMed: 11152458]

12. Yu XC, Margolin W. EMBO J 1997;16:5455–5463. [PubMed: 9312004]

13. Lu C, Erickson HP. Methods Enzymol 1998;298:305–313. [PubMed: 9751890]

14. Barshop BA, Wrenn RF, Frieden C. Anal. Biochem 1983;130:134–145. [PubMed: 6688159]

15. Zimmerle CT, Frieden C. Biochem. J 1989;258:381–387. [PubMed: 2705989]

16. Frieden C. Methods Enzymol 1994;240:311–322. [PubMed: 7823836]

17. Dang Q, Frieden C. Trends Biochem. Sci 1997;22:317. [PubMed: 9270307]

18. Mukherjee A, Lutkenhaus J. J. Bacteriol 1999;181:823–832. [PubMed: 9922245]

19. Correia JJ, Baty LT, Williams RC Jr. J. Biol. Chem 1987;262:17278–17284. [PubMed: 2826416]

20. Romberg L, Mitchison TJ. Biochemistry 2004;43:282–288. [PubMed: 14705956]

21. Sossong TM, Brigham-Burke MR, Hensley P, Pearce KH. Biochemistry 1999;38:14843–14850. [PubMed: 10555966]

22. Rivas G, Lopez A, Mingorance J, Ferrandiz MJ, Zorrilla S, Minton AP, Vicente M, Andreu JM. J. Biol. Chem 2000;275:11740–11749. [PubMed: 10766796]

23. Redick SD, Stricker J, Briscoe G, Erickson HP. J. Bacteriol 2005;187:2727–2736. [PubMed: 15805519]

24. Mingorance J, Rueda S, Gomez-Puertas P, Valencia A, Vicente M. Mol. Microbiol 2001;41:83–91. [PubMed: 11454202]

25. Scheffers DJ, Den Blaauwen T, Driessen AJM. Mol. Microbiol 2000;35:1211–1219. [PubMed: 10712701]

26. Mukherjee A, Saez C, Lutkenhaus J. J. Bacteriol 2001;183:7190–7197. [PubMed: 11717278]

$$P \underset{k_{-1}}{\overset{k_1}{\rightleftharpoons}} Z \qquad \textit{Monomer \quad activation}$$

$$Z + Z \underset{k_{-2}}{\overset{k_2}{\rightleftharpoons}} Z_2 \qquad \textit{Nucleation}$$

$$Z_2 + Z \underset{k_{-3}}{\overset{k_3}{\rightleftharpoons}} Z_3 \qquad \textit{Elongation}$$

$$Z_3 + Z \underset{k_{-4}}{\overset{k_4}{\rightleftharpoons}} Z_4$$

$$Z_4 + Z \underset{k_{-5}}{\overset{k_5}{\rightleftharpoons}} Z_5$$

$$Z_5 + Z \underset{k_{-6}}{\overset{k_6}{\rightleftharpoons}} Z_6$$

$$Z_6 + Z \underset{k_{-7}}{\overset{k_7}{\rightleftharpoons}} F$$

$$F + Z \underset{k_{-8}}{\overset{k_8}{\rightleftharpoons}} F \qquad \textit{Elongation}$$
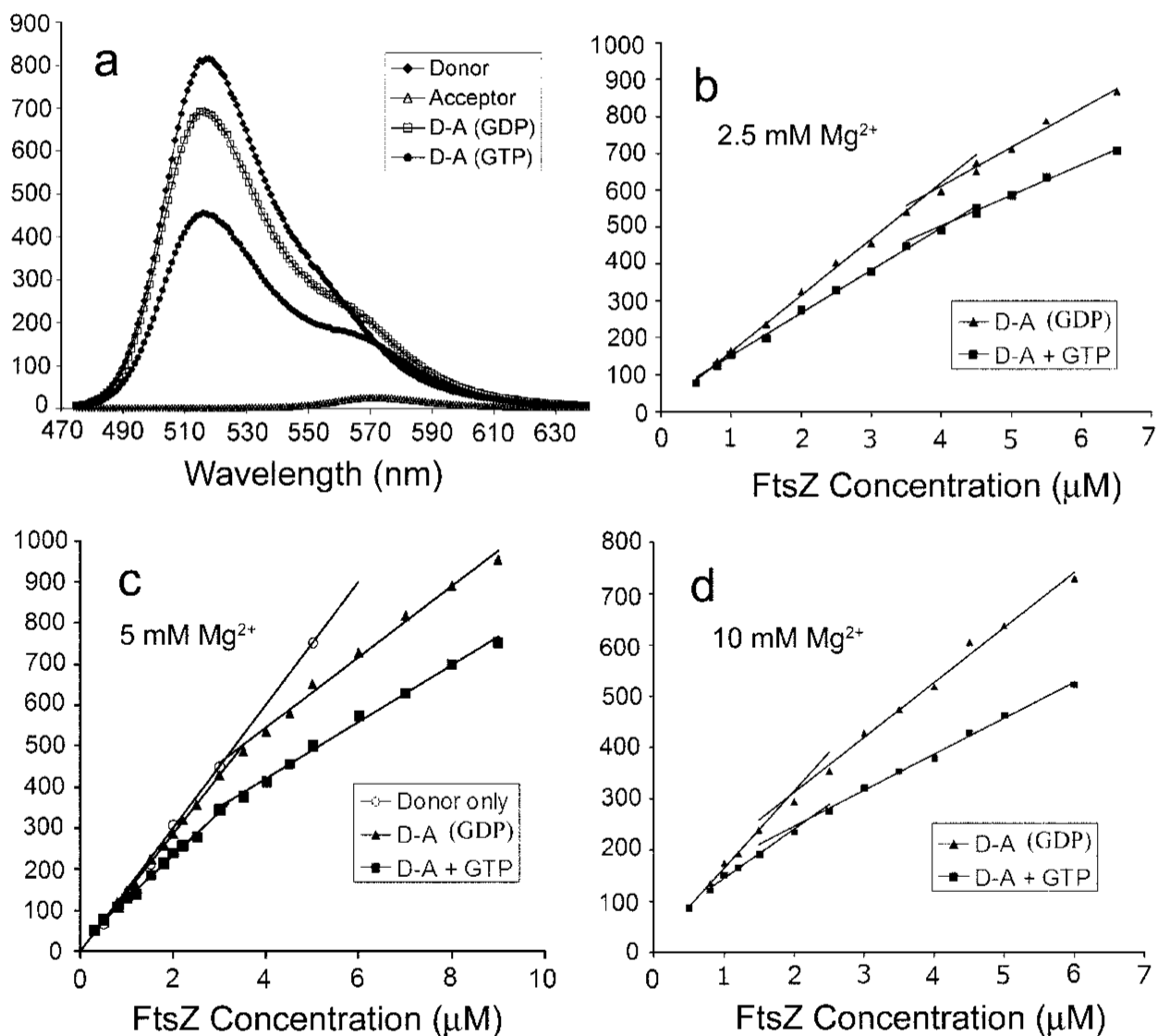
Scheme I.

Fig. 1. FRET assay of FtsZ assembly

a, the spectra of donor only, acceptor only, donor-acceptor (*D-A*) without GTP, and donor-acceptor with GTP. FtsZ was at 6 μ_M, and spectra were recorded 5 min after mixing. *b—d*, the donor fluorescence of FtsZ recorded at 516 nm is plotted *versus* the concentration of FtsZ. The three curves show different concentrations of Mg^{2+}: 2.5 m$_M$ (*b*), 5m$_M$ (*c*), and 10 m$_M$ (*d*).
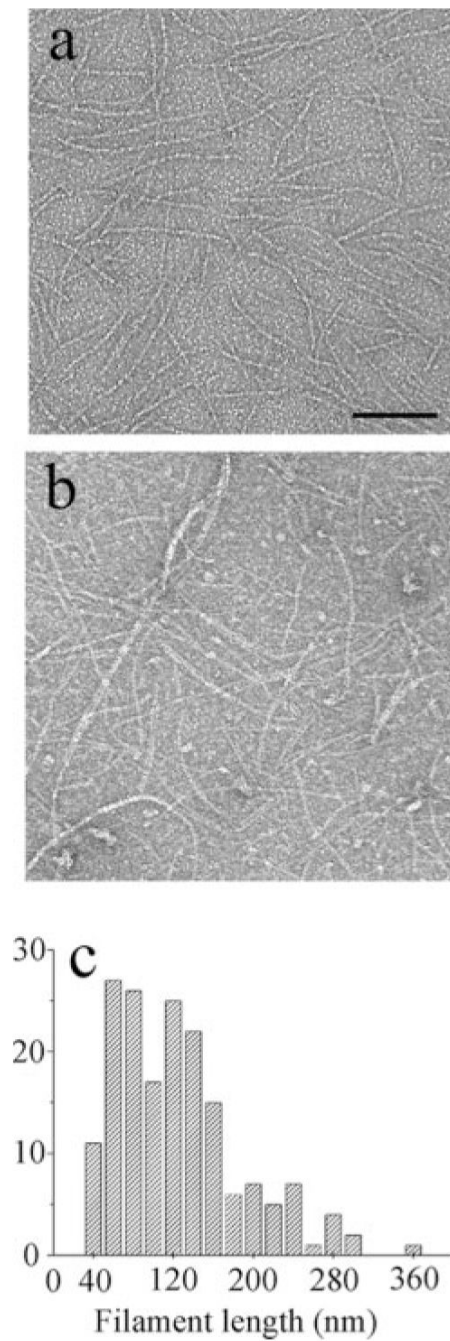
Fig. 2.
a and *b*, negatively stained EM images are shown of FtsZ-F268C at 2 μM (*a*) and 10 μM (*b*) in MMK buffer following 3 min of assembly. Protofilaments are almost all single-stranded at 2 μM, but at 10 μM, some are associated in pairs or small bundles (*bar* = 100 nm). *C*, the length distribution of FtsZ filaments assembled as in *a* is shown. The majority of filaments are in the range of ~80–160 nm or ~20–40 subunits.
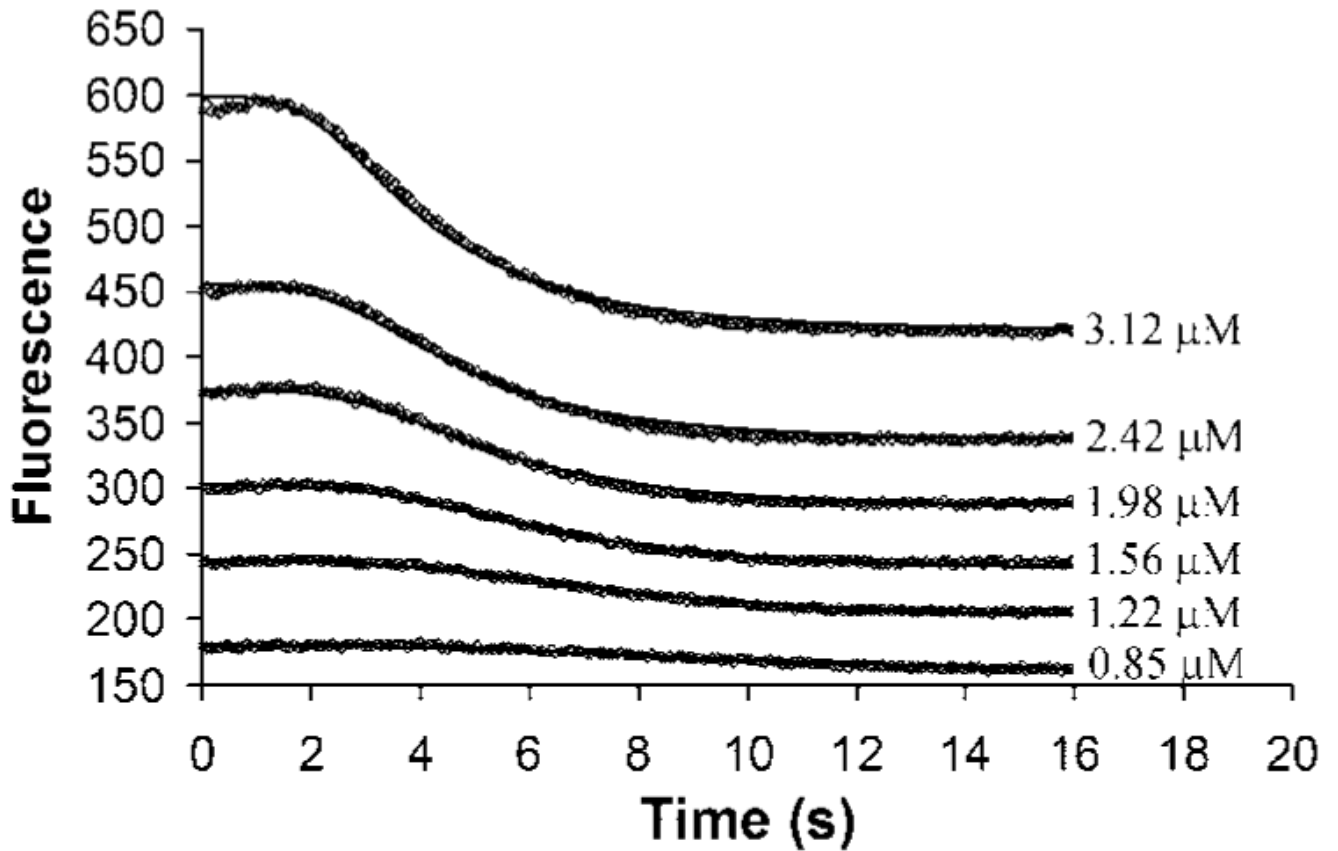
Fig. 3. The kinetics of FtsZ initial assembly detected by FRET
Assembly was initiated in the stopped-flow device by mixing with GTP, giving the indicated concentrations of FtsZ. The *solid lines* show the fitting to the dimer nucleation model.
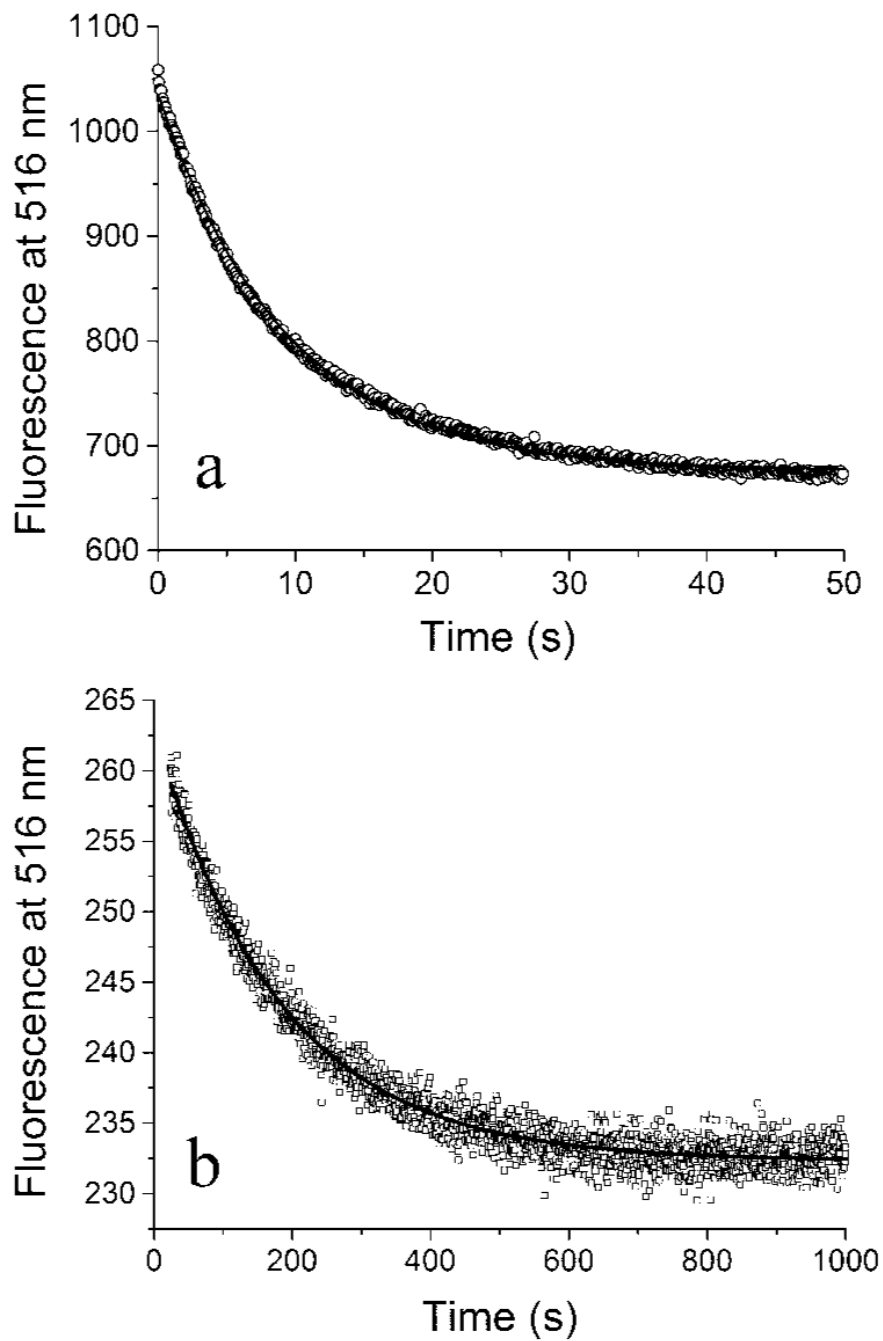
Fig. 4. The kinetics of subunit exchange when pools of preassembled donor and acceptor FtsZ protofilaments were mixed in 5m$_M$ Mg^{2+} (*a*) or in 2.5 m$_M$ EDTA (*b*)
Note the longer time scale in *b*. The curves are fits with a single exponential (decay constant 9.3 and 127 s with and without Mg^{2+}). FtsZ was at 6 $\mu$$_M$.
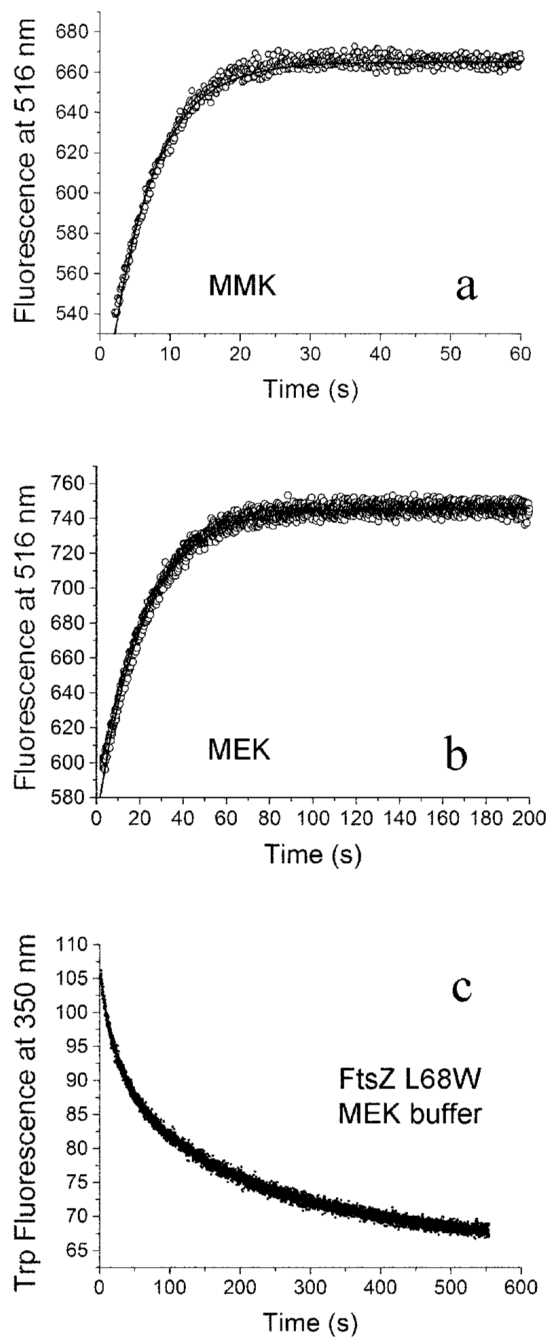
Fig. 5. The disassembly kinetics of FtsZ polymer following the addition of excess GDP
a, in MMK buffer, the decay constant for disassembly is 6 s. *b*, in MEK buffer, the decay constant for disassembly is 21 s. *c*, the disassembly of FtsZ-L68W assayed by the decrease in tryptophan fluorescence. The average decay constant is ~120 s. FtsZ was at 6 μM.

TABLE I

FtsZ assembly rate constants in two different buffers

Both buffers contain Mg^{2+}, and they differ in pH. The rates from the present FRET assay are compared with those obtained previously for FtsZ-L68W. k_1 and k_{-1} are the parameters for monomer activation, k_2 and k_{-2} are for formation of the dimer nucleus, and k_e and k_{-e} are for elongation.

Protein	Buffer	k_1	k_{-1}	k_2	k_e	k_{-2}	k_{-e}	k_{-2}/k_2	k_{-e}/k_e
		s^{-1}	s^{-1}	$\mu M^{-1} s^{-1}$	$\mu M^{-1} s^{-1}$	s^{-1}	s^{-1}	μM	μM
FtsZ-F268C	HMK	0.38	0.01	0.72	6.63	199.6	4.0	277.2	0.60
	MMK	0.38	0.01	0.79	6.60	199.8	3.48	252.9	0.53
FtsZ-L68W	HMK	0.70	0.04	1.02	3.61	1.23	0.36	1.21	0.10
	MMK	0.76	0.11	0.62	3.01	0.30	0.60	0.47	0.20